APPLICATION OF THE CRITICAL VOLTAGE EFFECT TO ALLOY STUDIES

C. G. Shirley, Motorola, Inc., Semiconductor Research and Development Laboratories, 5005 E. McDowell Rd., Phoenix, Arizona 85008, USA

R. M. Fisher, U. S. Steel Corp., Research Laboratory, Monroeville, Pennsylvania 15146, USA

Introduction

At certain accelerating voltages, Vc, greater than about 100 kV, diffraction patterns from precisely oriented thick single crystals show vanishing second order Kikuchi lines and other characteristic changes. The values of Vc depend sensitively on structure factors. Ever since the discovery of the effect[1,2] the critical voltage has been used to determine crystal parameters which influence structure factors. The simplest examples of this are refinements of low-angle scattering factors and Debye temperatures in pure metals.[3]

The information obtainable from a critical voltage measurement is much the same as that obtainable from X-ray measurements of Bragg reflection intensities. However, whereas X-ray measurements require a macroscopic volume of material, critical voltage measurements can be made on small volumes of crystal, 1 μm or less in diameter. Moreover, the image is available to select the area to study. This is especially useful in alloy studies because it is difficult to prepare large single crystals of any particular alloy, whereas it is relatively simple to produce polycrystalline alloys.

For any given alloy or metal there are usually only one or two accessible critical voltages to analyse. This is a problem for alloys since there are more parameters influencing the structure factors (e.g. composition, long-range order (l.r.o.), short-range order (s.r.o.) than for pure metals. Thus, analysis of alloy critical voltage data requires a simple, universal few-parameter model which describes the main influences on the structure factors. In this paper we present model expressions for the structure factors of ordered and disordered alloys based on the f.c.c. and b.c.c. structures, and we demonstrate their application to the analysis of critical voltage data.

Theory

The various crystal parameters affect Vc only through the structure factors, and once the structure factors are known it is relatively simple to use n-beam diffraction theory[4] to compute Vc. The emphasis here is therefore on the structure factors.

(a) Solid solutions.[5] The structure factor for a disordered solid solution is

$$f = m_A f_A \exp(-M_A) + m_B f_B \exp(-M_B) \tag{1a}$$

where

$$M_A = (8\pi^2/3) \; \langle u^2 \rangle_A \; s^2 \tag{1b}$$

and similarly for M_B. Here $s = (\sin\psi)/\lambda$, where ψ is the Bragg angle and λ is the electron wavelength. The mole fraction of A-atoms (or B-atoms) is m_A (or m_B), their mean-square displacements (m.s.d.) are $\langle u^2 \rangle_A$ (or $\langle u^2 \rangle_B$), and the atomic scattering factors in the alloy are f_A (or f_B). It can be shown that the m.s.d. can be decomposed into an average and a deviation from average:

$$\langle u^2 \rangle_A = \langle u^2 \rangle + (2m_B)^{-1} \langle \sigma u^2 \rangle \tag{2a}$$

$$\langle u^2 \rangle_B = \langle u^2 \rangle - (2m_A)^{-1} \langle \sigma u^2 \rangle \tag{2b}$$

where the ensemble averages are over squares of displacements irrespective of site occupancy (first terms) or over squares of displacements multiplied by a "spin" operator defined such that $\sigma_i = (2m_B, -2m_A)$ for an (A,B) atom on site i. Expressions for $\langle u^2 \rangle$ and $\langle \sigma u^2 \rangle$ may be further decomposed according to

$$\langle u^2 \rangle = \langle u^2 \rangle_t + \langle u^2 \rangle_s \tag{3a}$$

$$\langle \sigma u^2 \rangle = \langle \sigma u^2 \rangle_t + \langle \sigma u^2 \rangle_s \tag{3b}$$

The subscript t indicates the thermal components, while s indicates the static component due to atomic size disparity in alloys. For pure metals, the only non-zero term is $\langle u^2 \rangle_t$ whereas for solid solutions $\langle u^2 \rangle_s$ and $\langle \sigma u^2 \rangle_s$ can be quite large. The term $\langle \sigma u^2 \rangle_t$ is always small compared to the others and will be taken as zero in the models below.

For disordered solid solutions a useful model for the thermal contributions is

$$\langle u^2 \rangle_t = \frac{9\hbar^2}{\kappa A} \left\{ \frac{T\phi(\theta/T)}{\mu\theta^2} + \frac{1}{4\theta^2} \right\} \tag{4}$$

and $\langle \sigma u^2 \rangle_t = 0$. In (4), $\hbar$ is Planck's constant, κ is Boltzmann's constant, A is the atomic mass unit, ϕ is Debye's function, θ is the Debye temperature and $\mu = m_A\mu_A + m_B\mu_B$ where μ_A and μ_B are the pure metal atomic weights. Krivoglaz[6] has shown that for a mass-disordered alloy the error in approximating it to a pure metal with average mass is only a few percent even at T = 0. Thus, although the model in Ref. 5 was derived for $T>\theta$, extrapolation to $T<\theta$ using Equation (4) is not likely to introduce serious error. The alloy Debye temperature is given by

$$\mu\theta^2 = m_A\mu_A\theta_A^2 + m_B\mu_B\theta_B^2 + (\tau-1)(1-\alpha_1)m_Am_B(\mu_A\theta_A^2 + \mu_B\theta_B^2) \tag{5}$$

where α_n is the n^{th} neighbor Cowley-Warren s.r.o. parameter, and τ is an empirical parameter with the following physical interpretation:

$$\tau = 2\, g_{AB}/(g_{AA} + g_{BB}) \tag{6}$$

where g_{AA}, etc. are the spring constants connecting A-A, etc. atom pairs. τ is unity when g_{AB} is the arithmetic mean of g_{AA} and g_{BB}.

It is possible to compute contributions due to static displacements by computing sums over displacement fields. This procedure gives[5]

$$\langle u^2 \rangle_s = \frac{1}{4} m_Am_B\gamma^2a^2\eta^2 \left(Co + \sum_{n=1}^{\infty} C_n\alpha_n\right) \tag{7}$$

$$\langle \sigma u^2 \rangle_s = \frac{1}{2} m_Am_B(m_A-m_B)\gamma^2a^2\eta^2 \sum_{n=1}^{\infty} D_n\alpha_n \tag{8}$$

where values of C_n and D_n are given in Table I, where $\eta = d\ \ln a/dm_A$, a is the lattice parameter and γ is to be regarded as an empirical parameter of order unity.

Table I. Coefficients of Lattice Sums in Eqs. (7) and (8)

	f.c.c.		b.c.c.	
n	C_n	D_n	C_n	D_n
0	0.533	-	2.837	-
1	3.163	0.3485	2.123	1.464
2	0.926	0.0003	1.422	0.4015
3	2.413	0.0614	-2.431	0.1234

Notice that for vanishing s.r.o. $\langle u^2 \rangle_A = \langle u^2 \rangle_B$, that is, an atom's m.s.d. depends on its environment, not on its identity.

(b) Ordered alloys. The same kind of model can be developed for ordered alloys by taking into account the distinct sublattices. The additional parameter for ordered alloys is the long-range order parameter, S, which describes how atoms are distributed among the sublattices. Short-range order can also exist, but for simplicity we shall assume that it vanishes in the following. This assumption can be shown to imply that the m.s.d. depends only on the sublattice, not on the particular type of atom occupying a site in it.

(1) βCuZn structure. Assuming that m.s.d. depend only on the sublattice, the structure factors are given by[7]

$$F = \bar{f}\,(e^{-M_\alpha} + e^{-M_\beta}) + \frac{1}{2}\Delta f S\,(e^{-M_\beta} + e^{-M_\alpha}) \quad \text{(fundamental)} \tag{9a}$$

$$F = \bar{f}\,(e^{-M_\beta} - e^{-M_\alpha}) + \frac{1}{2}\Delta f S\,(e^{-M_\alpha} - e^{-M_\beta}) \quad \text{(superlattice)} \tag{9b}$$

where $\bar{f} = m_A f_A + m_B f_B$, $\Delta f = f_B - f_A$ and

$$M_\alpha = (8\pi^2/3)\,\langle u^2 \rangle_\alpha\, s^2$$

and similarly for M_β. The m.s.d. on the α and β sublattices may be decomposed into thermal and static components as

$$\langle u^2 \rangle_\alpha = \langle u^2 \rangle_{\alpha t} + \langle u^2 \rangle_{\alpha s} \tag{10a}$$

$$\langle u^2 \rangle_\beta = \langle u^2 \rangle_{\beta t} + \langle u^2 \rangle_{\beta s} \tag{10b}$$

The thermal components are given by

$$\langle u^2 \rangle_{\alpha t}^{-1} = \langle u^2 \rangle_\beta^{-1} = m_A R_A + m_B R_B + (\tau - 1)(m_A m_B + \frac{1}{4} S^2)(R_A + R_B) \tag{11}$$

where R_A and R_B are the reciprocal (thermal) m.s.d. of the pure elements at the same temperature as the alloy. Static components are given by

$$\langle u^2 \rangle_{\alpha s} = \frac{1}{16}\,\gamma^2 a^2 \eta^2\,(1.766\, g_1 + 1.071\, g_2) \tag{12a}$$

$$\langle u^2 \rangle_{\beta s} = \frac{1}{16}\,\gamma^2 a^2 \eta^2\,(1.071\, g_1 + 1.766\, g_2) \tag{12b}$$

where

$$g_1 = 4\, m_A m_B - 2(m_B - m_A)S - S^2$$

$$g_2 = 4\, m_A m_B + 2(m_B - m_A)S - S^2$$

Notice that in the limit as $S \to 0$ these expressions reduce to the b.c.c. zero s.r.o. case discussed above. Thus, γ and τ for the disordered alloy might be expected to be the same for the ordered alloy. For the βCuZn structure S must satisfy $0 \leq S \leq S_{max}$ where $S_{max} = 2m_B$ $(m_B < \frac{1}{2})$ or $S_{max} = 2m_A$ $(m_B > \frac{1}{2})$.

(2) Cu_3Au structure. For a B_3A alloy in which m.s.d. depend only on the sublattice (i.e. zero s.r.o.)

$$F = \bar{f}\,(3e^{-M_\beta} + e^{-M_\alpha}) + \frac{3}{4}\Delta f S\,(e^{-M_\beta} - e^{-M_\alpha}) \quad \text{(fundamental)} \tag{13a}$$

$$F = \bar{f}\,(e^{-M_\beta} - e^{-M_\alpha}) + \frac{1}{4}\Delta f S\,(3e^{-M_\alpha} + e^{-M_\beta}) \quad \text{(superlattice)} \qquad (13b)$$

where $M_\alpha = (8\pi^2/3) < u^2 >_\alpha S^2$, etc. With sublattice m.s.d. decomposed as in Eq. (10), we have for the thermal components

$$< u^2 >^{-1}_{\alpha t} = m_A R_A + m_B R_B + \frac{1}{4} S(R_A - R_B) + (\tau - 1)(m_A m_B + \frac{1}{4} S(m_B - m_A) + \frac{3}{16} S^2)(R_A + R_B) \qquad (14a)$$

$$< u^2 >^{-1}_{\beta t} = m_A R_A + m_B R_B - \frac{1}{12} S(R_A - R_B) + (\tau - 1)(m_A m_B - \frac{1}{12} S(m_B - m_A) + \frac{1}{48} S^2)(R_A + R_B) \qquad (14b)$$

where R_A and R_B are the reciprocal pure metal m.s.d. at the same temperature, and for the static components

$$< u^2 >_{\alpha s} = \frac{1}{4}\gamma^2\eta^2 a^2\,(0.0573\, g_1 + 0.4758\, g_2) \qquad (15a)$$

$$< u^2 >_{\beta s} = \frac{1}{4}\gamma^2\eta^2 a^2\,(0.1586\, g_1 + 0.3745\, g_2) \qquad (15b)$$

where

$$g_1 = m_A m_B + \frac{3}{4}(m_B - m_A)\, S - \frac{9}{16} S^2$$

$$g_2 = m_A m_B - \frac{1}{4}(m_B - m_A)\, S - \frac{1}{16} S^2$$

Again, these results reduce in the $S \to 0$ limit to the zero s.r.o. case of the f.c.c. solid solution so that γ and τ may be carried over from the disordered to the ordered case. In the B_3A alloy, S must satisfy $0 \leq S \leq S_{max}$ where $S_{max} = \frac{4}{3} m_B$ for $m_A > \frac{1}{4}$, and $S_{max} = 4\, m_A$ for $m_A < \frac{1}{4}$.

Models for any ordered alloy with structure based on the f.c.c. or b.c.c. lattice may be derived in the same way; in particular, using the dimensionless strain fields given by Shirley and Fisher.[5]

Applications

(a) Solid Solutions.

(1) FeCr. The atomic diameters of Fe and Cr differ by only 0.6% so that the static m.s.d. can be shown to be negligible. The room-temperature variation of Vc with composition shown in Figure 1 is well fitted by a single parameter, $\tau = 0.72$.[8] If Vc had been measured at two or more temperatures at each intermediate composition some measure of the outer electron redistribution on alloying (low-angle scattering factor changes) could have been obtained in addition to the Debye temperature variation. Alloys with negligible atomic radius mismatch are good candidates for outer electron redistribution studies using the Vc effect.

(2) NiAu (Ni-rich). These alloys have a large atomic radius disparity and there is a tendency to cluster (atoms prefer their own kind as nearest neighbors). Figure 2 shows the temperature variation of the total m.s.d. for an 17 mole %Au alloy.[9] The large static component is apparent. The best fit of the model to the data, assuming zero s.r.o., gives $\gamma = 1.23$ and $\tau = 1.87$. These values lead to the zero s.r.o. composition variation of thermal and static m.s.d. shown in Figure 3. The model may also be used to plot the m.s.d. vs. nearest neighbor s.r.o. as is shown in Figure 4 for a 30 mole %Au. We plot $\alpha_1 > 0$ since this corresponds to clustering. The negligible s.r.o. dependence of the thermal m.s.d. contrasts with the strong dependence of the static m.s.d. This is a general feature of f.c.c. alloys. In b.c.c. alloys the thermal m.s.d. also have weak s.r.o. dependence but the static m.s.d. have a weaker s.r.o. dependence than the f.c.c. alloys (see Table I). Increased m.s.d. generally reduce Vc, so clustering would tend to reduce Vc below the zero s.r.o. value. In Figure 5, the model with best-fit γ and τ is used to plot the

zero s.r.o. composition variation of Vc and $\partial Vc/\partial\alpha_1$. The room-temperature Vc data of Butler[10] and Lally[9] is superimposed on the plot in Figure 5, and agreement is good except for the 30 mole %Au point. The large depression in Vc (69 ± 17 kV) for this composition is due to a large degree of clustering s.r.o. which could not be quenched out because of the proximity of the spinodal. The $\partial Vc/\partial\alpha_1$ characteristic can be used to show that the Vc-depression is consistent with $\alpha_1 = 0.13 \pm 0.03$.

(3) CuAu. These alloys have a large atomic radius disparity, but in contrast to the NiAu alloys there is a tendency to order (atoms prefer the opposite kind as nearest neighbors). When the Vc data of Kuroda, Tomokiyo and Eguchi[11] is analyzed we find a best fit for $\gamma = 1.34$ and $\tau = 1.76$. The zero s.r.o. composition variation of the thermal and static m.s.d. is shown in Figure 3, and the variation with clustering s.r.o. ($\alpha_1 < 0$) of the m.s.d. components is shown in Figure 4. The best fit values of γ and τ were used in the model to plot the composition variations of Vc and $\partial Vc/\partial\alpha_1$ for the 400 and 222 critical voltages in Figures 6 and 7, assuming zero s.r.o. Superimposed on these theoretical curves are the data of Kuroda, et al.[11] and the earlier data of Sinclair, Goringe and Thomas[12] and of Thomas, Shirley, Lally and Fisher.[13] The fit is good except for the 400, 5%Au high-temperature data point which probably claims too small an error, and the triangular data points due to Sinclair, et al.[12] The triangular data point is higher than the zero s.r.o. model curve for both the 400 and 222 critical voltages. For the 400 Vc this increase is consistent with $\alpha_1 = -0.045 \pm 0.007$ while for 222 Vc it is $\alpha_1 = 0.051 \pm 0.007$. The agreement between the degree of ordering obtained from two different reflections is evidence for the validity of the model.

(b) Ordered Alloys.

(1) Cu_3Au. The models for ordered alloys discussed above formally reduce to the zero s.r.o. solid solution models as $S \to 0$. For an alloy which can be conveniently ordered and disordered, such as Cu_3Au, it is interesting to see how well the parameters determined in the solid solution predict the behavior in the ordered alloy. In addition to the solid solution data which was fitted by $\gamma = 1.34$ and $\tau = 1.76$ there are several data points for the ordered alloys.[12,13]

When the best-fit parameters for the disorderd alloy are substituted into Eqs. (14) and (15), the S-variation of the static and thermal m.s.d. for stoichiometric Cu_3Au at 300°K shown in Figure 8 is obtained. Notice that the Cu-rich and Au-rich sublattices do not have the same m.s.d. if $S \neq 0$. In contrast with the α-variation in disordered alloys, Figure 4, S-variation in the ordered alloy can cause a strong change in the thermal m.s.d. The Au-sublattice thermal m.s.d. decreases appreciably on ordering because in the ordered solid solution Au atoms are surrounded completely by Cu atoms and the Au-Cu spring constant is quite large compared with the like-atom spring constants ($\tau = 1.76$). The S-variation of the 400 and 222 critical voltages corresponding to the displacements of Figure 8 are given in Figure 9 along with existing data. It is important to note that both fundamental and superlattice structure factors depend strongly on S. This is why the 222 critical voltage varies almost as strongly with S, proportionally, as does the 400 critical voltage. It is also interesting to compare the composition variation of the m.s.d. and Vc for maximally ordered alloys of the Cu_3Au structure ($S = S_{max}$) with those for the disordered case ($S = 0$) since this gives the range of variation possible. The m.s.d. are given in Figure 10 while the corresponding critical voltages are given in Figure 11.

The lack of fit of the existing data to the model (Fig. 9) is most likely due to changes in atomic scattering factors on ordering. Both the 222 and especially the 400 critical voltages depend on values of the atomic scattering factors at low scattering angles. At low angles the atomic scattering factors are known to be quite sensitive to the arrangement of outer electrons. The 400 critical voltage is especially sensitive since it depends on the atomic scattering factor at the 100 reflection which occurs at a much lower angle than any existing data. The well-known role of valence electrons in the formation of the Cu_3Au II superlattice structure would indicate that outer electron rearrangements intrinsic to the ordered structure are likely.

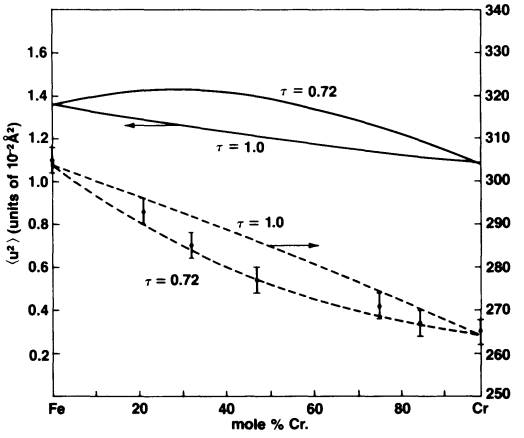

Fig. 1 - Room temperature thermal m.s.d. and 220 Vc for two values of τ. (Ref.8)

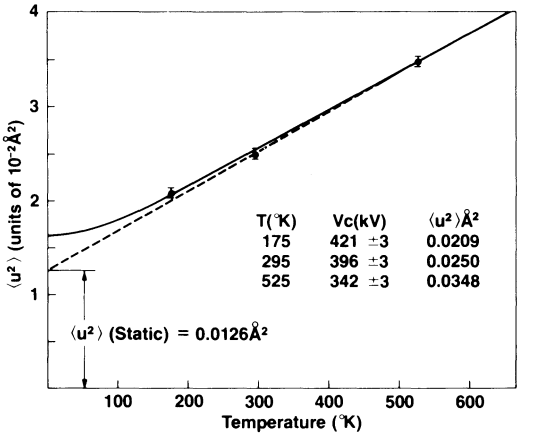

Fig. 2 - Total m.s.d. in Ni(83)Au solid solution vs. temperature from 400 Vc.

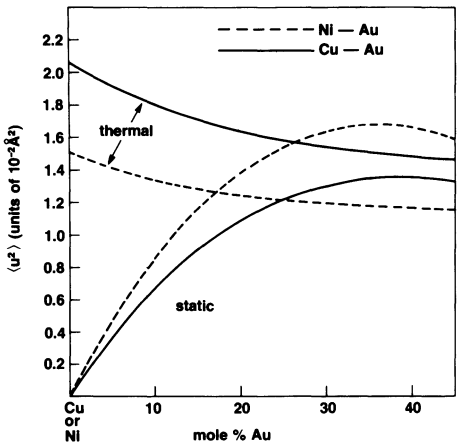

Fig. 3 - Static and thermal m.s.d. as a function of Au content in Ni-Au and Cu-Au solid solutions using best fit to Vc data. Zero s.r.o. assumed.

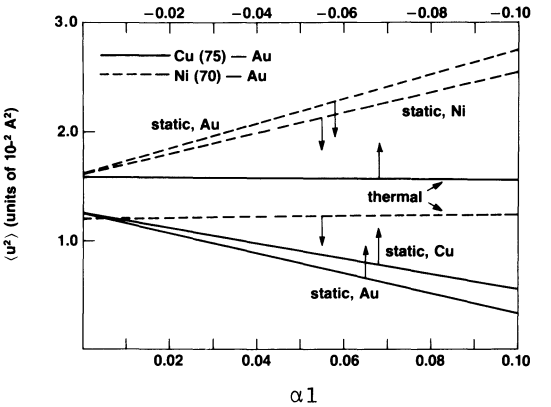

Fig. 4 - Static and thermal m.s.d. in Ni(70)Au and Cu(75)Au vs. clustering or ordering s.r.o., respectively.

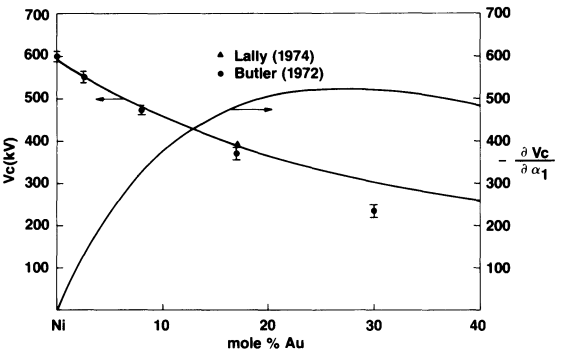

Fig. 5 - Room temperature 400 Vc composition variation in Ni-Au. Vc s.r.o. sensitivity is also shown.

Rocher, Sinclair and Thomas[14] used the temperature variation of the 400 critical voltage in the fully-ordered alloy (Thomas, et al.[13]) to compute changes in Cu and Au atomic scattering factors on ordering. To do this, they corrected for the thermal m.s.d. (static m.s.d. vanish, of course) by misapplying Eq. (5) to the *ordered* case. They should have used Eq. (14). At the time τ was unavailable and they would have used $\tau = 1$ as a best estimate. Now that a good estimate of τ is available it should be possible to obtain better estimates of the atomic scattering factor changes and to fit the data as well as Rocher, et al.[14] did. It is also possible that changes in γ and τ would occur on ordering. This is probably less likely than the atomic scattering factor changes since γ and τ depend more on core-core interactions which are less effected by ordering.

(2) βCuZn-structure alloys. Recent work of Fox[15] on β'NiAl and β'CoAl alloys shows that the data is fitted by values of γ rather higher than unity (for β'NiAl $\tau = 1.01$, $\gamma = 2.32$ and for β'CoAl $\tau = 1.35$, $\gamma = 5.63$). Fox noted that the Al-rich alloys must be handled by a model different from that for the βCuZn structure presented in the present paper since vacancies, not Al atoms, are the constitutional defects on the transition metal sublattice. For the Al-rich alloys he finds $\gamma \simeq 1$. It is not surprising that "vacancy-like" strain fields give $\gamma \simeq 1$ since the original model[5] was based on normalized theoretical strain fields around vacancies in b.c.c. alkali metals. On the other hand, the relatively larger strain fields in the transition metal-rich alloys, which correlates with binding energy and other properties, may indicate that the assumptions on which the model was based are violated in Ni- and Co-rich alloys. Nonetheless, even the transition-metal rich data can be well fitted by the model, and the parameters obtained are valid physical indices of the nature of the thermal and strain m.s.d. in the alloy.

References

1. F. Nagata and A. Fukuhara, Japan J. Appl. Phys. 6, 1233, 1967.
2. R. Uyeda, Acta Cryst. A24, 175, 1968.
3. J.S. Lally, C.J. Humphreys, A.J.F. Metherell and R.M. Fisher, Phil. Mag. 25, 321, 1972.
4. P.M.J. Fisher, Japan J. Appl. Phys. 7, 191, 1968.
5. C.G. Shirley and R.M. Fisher, Phil. Mag. 39, 91, 1979.
6. M.A. Krivoglaz, "Theory of X-ray and Thermal Neutron Scattering by Real Crystals," New York, Plenum, 1969.
7. B.E. Warren, "X-ray Diffraction," Addison-Wesley, 1969.
8. C.G. Shirley, J.S. Lally, L.E. Thomas and R.M. Fisher, Acta Cryst. A31, 174, 1975.
9. J.S. Lally, private communication, 1974.
10. E.P. Butler, Phil. Mag. 26, 33, 1972.
11. K. Kuroda, Y. Tomokiyo and T. Eguchi, in: Proceedings of 5th Int. Conf. on HVEM (Tokyo, Japanese Soc. of Electron Microscopy), 1977.
12. R. Sinclair, M.J. Goringe and G. Thomas, Phil. Mag. 32, 501, 1975.
13. L.E. Thomas, C.G. Shirley, J.S. Lally and R.M. Fisher, in: High-Voltage Electron Microscopy, 38 (London, Academic Press), 1974.
14. A. Rocher, R. Sinclair and G. Thomas, at Int. Conf. on High Voltage Electron Microscopy, Toulouse, France, 1975.
15. A. G. Fox, this conference.

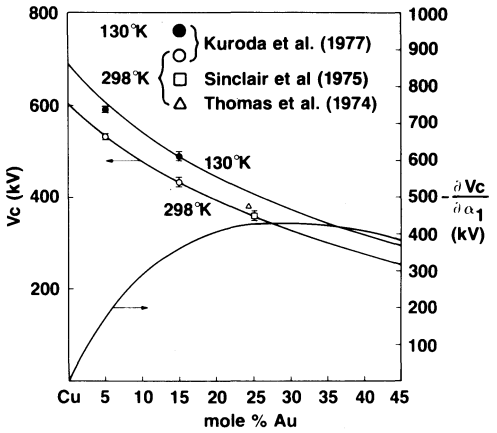

Fig. 6 400Vc

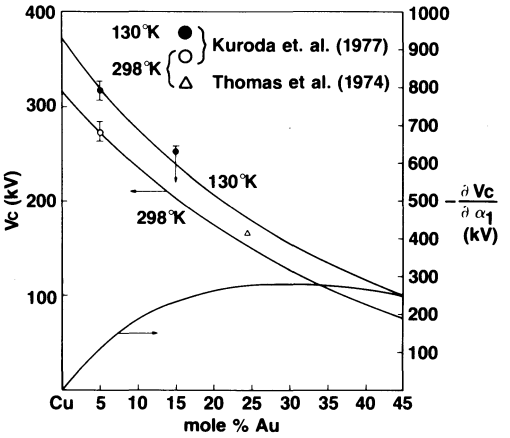

Fig. 7 222 Vc

Composition variation in Cu-Au. Vc s.r.o. sensitivity is also shown.

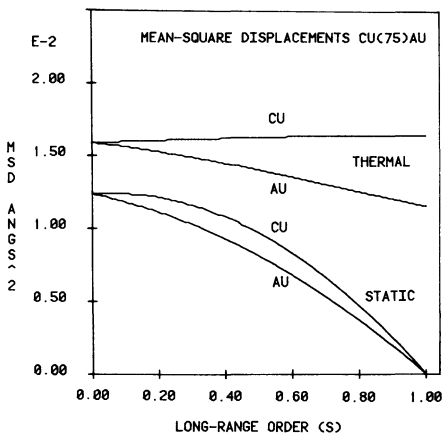

Fig. 8

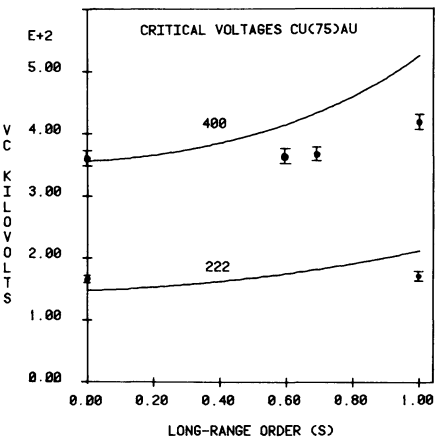

Fig. 9

Model calculations of thermal and static m.s.d. (Fig. 8) and Vc (Fig. 9) vs. long-range order for stoichiometric Cu_3Au.

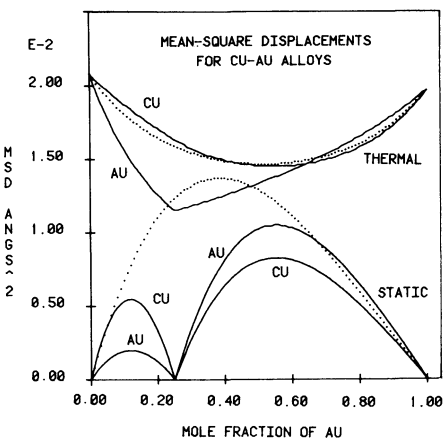

Fig. 10

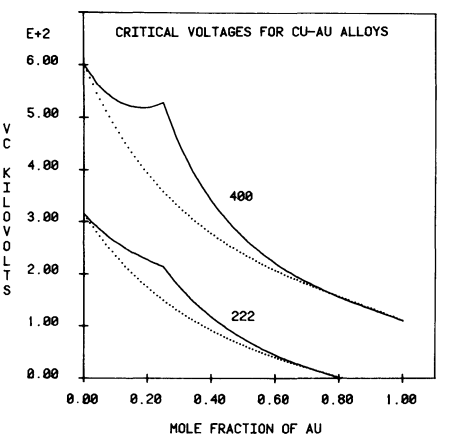

Fig. 11

Maximum l.r.o. composition variation of thermal and static m.s.d. (Fig. 10) and Vc (Fig. 11) (solid curves) compared with disordered alloys (dotted).